Lab on a Chip

Modular, Pumpless Body-on-a-Chip Platform for the Co-Culture of GI Tract Epithelium and 3D Primary Liver Tissue

Journal:	*Lab on a Chip*
Manuscript ID	LC-ART-04-2016-000461.R1
Article Type:	Paper
Date Submitted by the Author:	27-May-2016
Complete List of Authors:	Esch, Mandy; Syracuse University Ueno, Hidetaka; Kagawa University Applegate, Dawn; RegeneMed Shuler, Michael; Cornell University, Department of Chemical and Biomolecular Engineering

Modular, Pumpless Body-on-a-chip Platform for the Co-Culture of GI Tract Epithelium and 3D Primary Liver Tissue

Mandy B. Esch,[1,4] Hidetaka Ueno,[2] Dawn R. Applegate,[3] Michael L. Shuler[4,*]

1) Department of Biomedical and Chemical Engineering, 303 Bowne Hall, Syracuse University, Syracuse, NY,13224, United States

2) Kagawa University, Kagawa, Japan

3) RegeneMed Inc., 9855 Towne Centre Drive Suite 200, San Diego, CA 92121, United States

4) Department of Biomedical Engineering, 300 Kimball Hall, Cornell University, Ithaca, NY, 14853, United States

**) Corresponding author*

Keywords: Bioreactor, gravity-driven flow, microfluidic cell culture, microphysiological system, body-on-a-chip, primary liver cells, 3D co-culture, multi-organ microdevice, tissue chips, organ-on-a-chip

Abstract: We have developed an expandable modular body-on-a-chip design that allows for a plug-and-play approach. The design consists of single-organ chips that are combined with each other to yield the multi-organ body-on-a-chip system. Fluidic flow through the organ chips is driven via gravity and controlled passively via hydraulic resistances of the microfluidic channel network and a passive valve mechanism. Such pumpless body-on-a-chip devices are inexpensive and easy to use. We tested the device by culturing GI tract tissue and liver tissue within a pumpless body-on-a-chip device. Integrated Ag/AgCl electrodes were used to measure the resistance across the GI tract cell layer. The transepithelial resistance (TEER) reached values between 250 to 650 Ωcm^2 throughout the 14-day co-culture period. These data indicate that the GI tract cells retained their viability and the GI tract layer as a whole retained its barrier function. Throughout the 14-day co-culture period we measured low amounts of aspartate aminotransferase (AST, ~10-17.5 U/L), indicating low rates of liver cell death. Metabolic rates of hepatocytes were comparable to those of hepatocytes in single-organ fluidic cell culture systems (albumin production ranged between 3-6 μg/day per million hepatocytes and urea production ranged between 150-

200 µg/day per million hepatocytes). Induced CYP activities were higher than previously measured with microfluidic liver only systems.

Introduction:

In 2017, the use of animals for the purpose of drug testing in modern medicine reaches its 80-year anniversary.[1] Animal tests have been invaluable for predicting the potential adverse effects of drugs on humans. It is known, however, that not all drugs that are safe for animals are safe for humans, and that only about 10% of drugs that heal diseases in animals do so in humans as well.[2-4] Recent research has uncovered some of the reasons for these discrepancies.[5-11] One of the problems is that animal drug metabolism is not a good mimic of human metabolism.[8]

A much-discussed alternative to testing drugs is to create a the human metabolism from scratch, using in vitro tissues grown from human organs and connecting them with each other via fluidic channels. Within the last fifteen years several artificial multi-organ systems were developed,[12-24] and proof-of-concept experiments have shown that this strategy works.[13-21] These complex systems are called multi-organ microphysiological systems or body-on-a-chip systems (and before 2005 micro cell culture analogs, microCCAs). If operated with human tissues that represent the majority of the human body authentically, body-on-a-chip systems could, in the near future, change how we evaluate new drug candidates.[25]

The usefulness of body-on-a-chip systems for drug testing arises from the fact that we can combine several tissues with each other, and recirculate a common cell culture medium among the tissue compartments.[12-23] Recirculation in a physiologically relevant pattern allows metabolites generated in one tissue chamber to reach other tissues and react with them. Such devices can not only predict the actions of drugs on specific tissues, but also the effects of a drug's metabolites on the human body as a whole.[13-23,26]

Despite their potential usefulness, current body-on-a-chip systems are not yet being used in large-scale drug screening. The predictive power of the devices depends on the authenticity of tissue behavior, where tissues built from immortalized cell lines generally behave less authentically than those constructed from primary or stem cell sources. The introduction of on-chip fluid controls and growth factor reservoirs

can help provide unique environments for special tissues that are constructed from primary cells or stem cells. [12] However, active on-chip fluid controls make devices more complex and expensive. Many of these systems are also operated with pumps that can be expensive and are prone to introduce errors such as those caused by air bubbles and leaking of medium due to pressurization. We believe that a device that is modular and that controls fluidic flow passively is less expensive and suitable for highly parallel drug screening. Such devices will help in providing the benefits of body-on-a-chip systems to benefit many more patients than currently available systems.

Without the development of new types of devices that allow for highly parallel operation in an inexpensive way, the potential benefits of body-on-a-chip systems will remain limited to a few areas of medicine where costly screening is permissible. Here, we introduce a device design for body-on-a-chip systems that allows for inexpensive, highly parallel operation while providing the benefits of near physiologic design that is needed to mimic the human metabolism accurately. We re-designed a previously proposed pumpless systems[27] so that it achieves physiologically relevant medium streams through each tissue chamber. We accomplished this through adjusting the hydraulic resistances of each fluidic channel. In addition, we introduced a set of passive valves that direct fluidic flow through organ chambers in a unidirectional way (as opposed to bidirectional flow in previous devices). These strategies to passively control fluidic flow allow us to operate body-on-a-chip systems inexpensively and in large numbers. Unidirectional flow also enables us to include barrier tissues that are sensitive to the direction of shear.

In addition to passive fluid controls, we also implemented a modular approach with separate single tissue microfluidic chips that allow for individual tissue maturation separate from each other. We can use these single organ chips to conduct single organ tests, or to combine them with each other in a ‘plug-and-play’ approach in order to create a multi-organ system.

We demonstrate the operation of the devices that are controlled passively, provide unidirectional fluidic flow, and a modular design approach by co-culturing GI tract epithelium (a tissue that is sensitive to the direction of flow) with liver tissue that is constructed from primary parenchymal and non-

parenchymal cells (a tissue that requires maturation separate from other tissues). The goal of this work is to show that our new, inexpensive device performs as well as previously developed proof-of-concept devices that were operated with pressure-driven flow via peristaltic pumps, and with tissues derived from cell lines.[17,18] Compared to these previous devices, the current device design has the advantage of being modular, which allows us to operate it with more tissues that behave more authentically than those constructed from cell lines. Our device design also demonstrates how passive fluid controls can be used to create near-physiologic fluidic flow, making the devices suitable for inexpensive, highly parallel operation as would be needed for high throughput drug screening.

Materials and Methods:

1) Modular Design Approach

Since tissues constructed form primary cells require specialized growth conditions in order to mature, we developed a device design that allows us to culture each tissue (GI tract epithelium and liver) on a single-organ chip, and then combine these single-organ chips with each other. Each organ chip contains microfluidic channels that facilitate medium flow through the organ chamber at flow rates that mimic physiologic values, i.e. the flow rate of blood through a human tissue section the same size of the organ chamber. This design enabled us to mature GI tract tissue (16 days to maturation in modified DMEM) and human primary liver tissue (9 days in specialized liver medium) separate from each other before combining them for 14 days of co-culture (Fig. 1 and 2).

2) Organ Chamber Dimensions

Data for the sizes of human organs, blood flow through each organ, and blood distribution in the body were obtained from a collection of human data by Davies et al. and Price et al.[28,29] Organ chamber volumes in the device were calculated to be 1/95,000th of those of organ volumes. Final organ chamber volumes on each organ chip are 12.9 mm^3 for the GI tract chamber and 16.5 mm^3 for the liver chamber.

3) Microfluidic Channel Dimension

The two organ chips were constructed with each containing a fluidic circuit. The GI tract chip contained a fluidic channel that perfused the apical side of the GI tract epithelium, and the liver chip contained a fluidic channel that perfused the liver chamber as well as the basolateral side of the GI tract epithelium. When assembled into a multi-organ system the GI tract epithelium and liver were connected with each other through a porous membrane that allowed soluble metabolite exchange between the two tissues. The fluidic channel that supplied the liver chamber plus the basolateral side of the GI tract epithelium represents part of the body's systemic circulation of the human body, i.e. the medium in it is the blood surrogate. The medium in the apical chamber of the GI tract epithelium represents the liquid present in the GI tract lumen.

Medium flow within both organ chips of the device was driven via gravity. Height differences between inlets and outlets were created by placing the device on a rocker platform. Flow rates were controlled passively via the hydraulic resistances of the microfluidic channels on each organ chip. We designed the dimensions of each fluidic circuit so that the hydraulic resistances of all elements in it result in flow rate that is close to physiologic values, i.e. close to the flow rate of blood within a tissue section of the size of the organ chamber. In the human body, 14 microL of blood perfuse a liver volume of the size of 16.5 mm^3 per minute, and 10 microL of blood perfuse a GI tract volume of the size of 12.9 mm^3.

We used the following equations for the hydrostatic pressure drop between two connected reservoirs at a platform tilt angle of 18º (1), for the hydraulic resistances that are needed to achieve near physiologic flow rates within the organ chambers (2,3), and for the length, width and depth of channels that will provide the needed hydraulic resistance (4) to calculate channel dimensions for each organ chip:

(1) $\Delta P = \rho g h$ [Pa],

with ΔP being the pressure drop between inlet and outlet for a height difference h at a given platform tilting angle, with ρ being the density of cell culture medium in kg/mm3, and g being the gravity constant.

(2) $R=\Delta P/Q(\text{organ segment})$ [(Pa*s)/m3],

with R being the hydraulic resistance of the components of each microfluidic circuit (channels plus tissue chamber) and Q(organ, scaled) being the flow rate through 1/95,000 of the organ.

Given the hydrostatic pressure drop that occurs at a tilting angle of 18°, the sum of the hydraulic resistances present in each fluidic branch within each of the two fluidic circuits (one branch per organ, with each consisting of a cell culture chamber and microfluidic channels that lead to and away from it, and the channels that make up the valve capillaries) determine the flow rate:

(3) $Q(\text{organ, segment}) = \rho gh / (R(\text{channel in}) + R(\text{chamber}) + R(\text{channel out}) + R(\text{valve capillaries}))$ [L/min]

Since ΔP is determined by the density of cell culture medium and the platform tilt angle according to equation (1), the hydraulic resistance of the tissue culture chamber is given by its size, and the hydraulic resistance of the valve is given by the dimensions of the valve, one way to achieve the needed fluid flow rate is by adjusting the height, width and length of the microfluidic channels that supply each tissue chamber with medium.

(4) $R(\text{channels}) = [12\eta L/(1-0.63(h/w))] * (1/h3w)$

with η being the dynamic viscosity of cell culture medium, L being the length of the channel, h being the height of the channel, and w being the width of the channel (with $w > h$ for all channels). We kept channel lengths and heights constant for each chip and varied channel widths only to achieve the needed hydraulic resistance. In our system all channels were wider than high.

Since liquid levels in each of the reservoirs change over time (i.e. Δh changes over time), and we tilt the platform back and forth at time intervals of 60 seconds (i.e. not enough time for Δh to become zero), the flow rate does not reach steady state. We designed the device so that the flow rate averaged over 60 seconds is the flow rate (Qorgan segment) needed.

4) Valve Design

A passive valve mechanism without moving parts was designed and incorporated as part of the platform (Fig 3). This passive valve directs medium flow between two reservoirs that supply each of the two organ chips (two reservoirs supply the apical side of the GI tract tissue, and two separate reservoirs supply the systemic circulation, i.e. basolateral side of the GI tract tissue and liver tissue). The two reservoirs are connected with each other through two separate on-chip channels, one that leads medium through the organ chamber and a backflow channel. Medium flows through the organ chamber when the device is tilted in one direction (Fig. 4), and through the backflow channel when it is tilted in the other direction. During the back tilt, capillary forces inside the valve retain the fluid in the channels that supply the organ chamber and prevent it from flowing backwards. Once the platform tilts back into the first position, medium flows again through the organ chambers, but is held in the backflow channel via capillary forces.

5) Microfabrication

The platform and the two organ chips were designed with Solidworks (SolidWorks Corp., Waltham, MA, USA) and printed with a 3D object printer (ObJet 30Pro, Stratasys Ltd., Rehovot, Israel) using the provided Veroclear polymer. The printed devices were cured for 48 hours at 40 ºC under vacuum and then coated with 5g of parylene C using a coater from SCS Equipment (Dallas, TX, USA, Model PDS 2010 Labcoater). The platform consisted of two housing pieces (top and bottom) into which the two organ chips fit (Fig. 1 and 2). Once assembled the two organ chips are connected with the reservoirs and valve mechanism that supply medium at near physiologic flow rates.

Each of the two organ chips was assembled from two 3D printed polymer pieces. Porous polycarbonate membranes (Sterlitech Corp., catalog # P/N PCT45025100) were sandwiched between these two pieces. The GI tract tissue was cultured directly on this porous membrane on the assembled GI tract chip. On the liver chip, a woven nylon scaffold (RegeneMed, Inc.) was inserted above the porous polycarbonate membrane, providing the 3D culture environment for the liver tissue as previously described. [30]When the organ chips were stacked on top of each other in the platform, the porous

membranes enabled communication between the basolateral side of the GI tract tissue and the liver tissue, mimicking the close connection these two tissues experience in vivo.

6) GI tract Tissue Construction

Caco-2 cells were maintained in cell culture flasks using DMEM with 10% FBS at 37ºC and 5% CO2. 16 days prior to the assembly of the devices, the cells were lifted using trypsin and seeded onto the porous membrane of the GI tract chip at a concentration of 100,000 cells per cm2. The cell-loaded chips were placed into petri dishes and maintained for 16 days using DMEM with 10% FBS at 37ºC and 5% CO2.

7) Liver Tissue Construction

We constructed 3D liver tissues on liver chips using 3D scaffolds that were placed into the liver tissue culture chambers. The scaffolds were obtained from RegeneMed Inc. (San Diego, CA). They consist of two layers of interwoven polymer fibers that together create a 3D mesh structure. Primary human hepatocytes and non-parenchymal cells (a mixture of primary human fibroblasts, stellate cells, Kupffer cells, sinusoidal endothelial cells, and vascular and biliary epithelial cells) were obtained from Regenemed Inc. (San Diego, CA). Nine days prior to device assembly, non-parenchymal cells (NPC) were thawed and seeded onto 3D scaffolds that were placed in the organ chamber of the liver chips. The seeding concentration of NPC was 150,000 cells per liver chip. The chips with NPC cell cultures were then placed in petri dishes and maintained for 7 days in a humidified 5% CO2 incubator at 37°C to allow the NPC to express extracellular matrix proteins and growth factors necessary to support hepatocyte function. The cultures were sustained with medium obtained from RegeneMed Inc. (# L3SNB-500, RegenMed, San Diego, CA). On day 7 after NPC seeding, cryopreserved primary human hepatocytes were thawed and seeded onto the liver chip at a concentration of 250,000 cells per scaffold. After 48 h of maintaining these mixed cell cultures in petri dishes, the cell-loaded chips were ready for use with the device.

8) Device Assembly and Operation

When both GI tract and liver tissues were mature (Caco-2 cells after 16 days and 3D liver tissues after 9 days of on-chip culture in petri dishes) one of each of the GI tract and liver chips was aseptically transferred into the cavity of the bottom platform piece (Fig 1). The assembled devices were covered with sterilized lids and transferred onto a rocking platform that was placed into an incubator. The device was rocked back and forth every 60 seconds, facilitating perfusion by creating a height difference in liquid levels in each of the two sets of reservoirs. The rocking platform tilted between angles of ±18°, resulting in periodic, unidirectional, gravity-induced medium flow for 60 seconds in intervals of 120 seconds.

Prior to transfer, the two platform pieces were sterilized with 70% ethanol for 24 hours and washed with PBS. The device was filled with cell culture medium and closed without encapsulating air bubbles using the top piece. We filled the two wells that supplied the apical side of the GI tract tissue with 150 microL of Caco-2 medium (DMEM with 10% FBS), and the two wells that supplied the systemic circulation circuit with 150 microL of liver cell medium (# L3SNB-500, RegenMed, San Diego, CA). We renewed medium in all four reservoirs (150 microL) every day for 14 days and analyzed the medium recovered from the systemic circulation circuit for metabolites produced in the liver (urea and albumin) and for liver viability markers (AST).

9) Liver Cell Viability

To determine the viability of liver cells throughout the 14-day co-culture period we measured the amounts of aspartate aminotransferase, (AST, a cytosolic enzyme) in the medium taken from the systemic circulation loop of the device. Testing was performed at the clinical pathology laboratory in the Animal Health Diagnostic Center at Cornell University, using an automated chemistry analyzer (Hitachi Modular P, Roche Diagnostics) with manufacturer's reagents. Measuring AST levels allows us to quantify the amount of liver cell death that occurred over the period of time between measurements [18] and express albumin and urea production per number of live liver cells.

10) TEER Measurements

GI tract tissue function can be measured via the transepithelial cell layer resistance (TEER). For the purpose of conducting these measurements on-chip throughout the 14-day co-culture period, we integrated custom-made Ag/AgCl electrodes into the cell culture platform (Fig. 2). The electrodes were constructed from 3 mm thick, hollow silver tubes and silver chloride electrodes purchased from A-M Systems (Sequim, WA catalog #550008). We used a World Precision Instrument (Millicell ERS-2) to measure the TEER daily after combining GI tract and liver tissues with each other.

It should be noted that the electric field produced in custom-made systems can differ from that produced in commercially available measuring cups. TEER values measured with custom-build systems cannot not be directly compared to those measured with commercial cups. Further, since the second TEER electrode is located beneath the liver tissue we conducted control measurements, finding that the liver scaffold and tissue do not contribute to the TEER value, i.e. the reading without GI tract tissue is zero.

11) Rates of Urea and Albumin Synthesis

200 μL of cell culture medium (100 μL from each well) were collected from the systemic circulation circuit of the devices on day 3, 7, 10 and 14 of the co-culture with day 1 corresponding to the first day of co-culture in the device. Urea concentrations in the medium were measured using a DIUR assay kit, which we used as suggested by the manufacturer (BioAssay Systems, Hayward, CA, USA, QuantiChrom catalog #DIUR-500). In short, we transferred 50 μL of medium into the wells of a 96 well plate, added chromogenic reagent that forms a stable colored complex specifically with urea, and measured the optical density of the solution within 5 minutes of adding the chromogenic reagent at 520 nm using a spectrophotometer. The results were compared to a standard curve and are expressed as μg/day/million cells.

Albumin synthesis was evaluated by Enzyme-Linked Immunosorbent Assay (ELISA), using a kit

and following the manufacturer's directions (Bethyl Laboratories, Inc., Montgomery, TX, USA, catalog # E80-129). In short, we coated the wells of a 96-well plate with goat anti-human albumin antibody and washed the wells with buffer. We then transferred 100 μL medium taken from the cell culture devices into the wells. After incubation, we added HRP-conjugated goat anti-human antibody to the wells and incubated for 1 hour. Following a washing step with buffer, we added 100 μL of enzyme substrate (tetramethylbenzidine) and incubated for 15 min. After adding stopping solution, we measured the absorbance of the solution using a plate reader at 450 nm.

12) P450 Enzyme Activity

CYP450 enzyme activity in the liver chip was monitored throughout the 14-day co-culture period using Promega Glo assays (Promega Corp., Madison, WI, USA, catalog #V9002 for CYP3A4 and catalog #V8752 for CYP1A1). These non-destructive assays allow repeat CYP450 induction measurements on the same cultures over time. Briefly the induction reagent (10 μM of rifampicin for CYP3A4 and 1 μM of 3-methyl-cholanthrene for CYP1A1 induction) was diluted in medium and added to the two reservoirs that served the systemic circulation circuit for 72 hours. We then washed the reservoirs with buffer three times for 5 minutes and subsequently replaced the buffer with IPA-luciferin. We used separate devices for measuring the induction of each enzyme. At the end of the incubation period, medium was collected and transferred into the wells of a 96 well-plate. Detection reagent was added and luminescence was read with a Veritas luminometer using the settings provided by the manufacturer. Results were expressed as multiples of the level of induction observed in vehicle controls without induction reagents.

13) Statistical Analysis

Each data point plotted in graphs represents the mean of three separate experiments ± standard deviation. Multiple means were compared with a one-way ANOVA, followed by a Bonferroni correction for the number of pair-wise comparisons (JMP software). Comparison of two values with each other was

performed using Student's t-tests. A p value of < 0.05 was considered significant.

Results:

1) Passive Device Operation

The device was designed so that the fluidic flow through each of the two organ chambers was controlled via the hydraulic resistances of the microfluidic circuits. To determine the medium flow rate experimentally, we measured the average flow rate when the device was tilted at and angle of +18º and medium flowed through the organ chambers. At a constant tilting angle at +18º flow rates change over the course of 60-seconds for which the angle is held. The device is then tilted on a rocker platform in the other direction for 60 seconds to refill the inlet reservoir with medium. The liquid levels in each of the reservoirs change over the course of the 60-second hold time, meaning that Δh between the liquid levels in the two reservoirs changes over time. The flow rate does not reach steady state and we measured the average flow rate over 60 seconds. The average flow rate was 20.5 ± 0.7 μL/min for the blood surrogate (i.e. cell culture medium) in the systemic circulation circuit, supplying the basolateral GI tract chamber and liver chamber, and 24.5 ± 0.9 μL/min in the apical GI tract chamber.

The total medium volume in the systemic circulation circuit represents the blood volume of the human body, scaled by a factor of 95,000 (this volume is 61.3 μL), plus additional liquid that is required to operate the device (this additional volume is 260 μL). It is our goal to decrease the amount of additional liquid in the device so that eventually the liquid-to-cell-volume reaches physiologic levels.

2) Device Performance: Liver Cell Viability

Throughout the 14-day co-culture period in our device liver cells were exposed to any substances Caco-2 cells released via the porous membrane into the basolateral compartment, i.e. the systemic circulation part of the device. Medium was recovered from the systemic fluidic circuit and analyzed for the cytosolic enzyme aspartate aminotransferase (AST). Throughout the 14-day co-culture period we measured low amounts of AST (~10 - 17.5 U/L) (Fig.5A), indicating high cellular viability in the liver

tissue as discussed in Esch et al.[18] This high level of liver cell viability was maintained for the 14-day duration of the co-culture within the platform (Fig 5A).

3) GI tract Epithelium Integrity: TEER Measurements

The transepithelial resistance of the Caco-2 layer gives us information about the cell's performance as a barrier tissue. The measured TEER under unidirectional medium flow was lowest right after device assembly and then rose over time from ~250 Ohms*cm2 to about ~650 Ohms*cm2 (Fig. 5B). Under bidirectional medium flow, TEER values dropped to zero after 48 hours of device operation (Fig. 5B). Since Caco-2 cells are sensitive to the direction of flow, the performance of the integrated valves can be judged by the TEER. The observed results provide evidence for the assumption that under unidirectional flow the cells maintained their barrier function throughout the 14-day co-culture period. We observed a relatively high variability when measuring TEER, perhaps reflecting slightly different degrees of cell layer maturity at the point of device assembly.

4) Albumin and Urea Production

To assess the metabolic activity of the liver tissue when co-cultured with GI tract tissue for 14 days, we measured concentrations of albumin and urea in the medium recovered daily from the systemic circulation circuit. We estimated the albumin and urea production per million hepatocytes per day. We found that the cells produced albumin at an average rate of 3-6 μg/million cells per day, and urea at an average rate of 150-200 μg/million cells per day (Fig. 6 A and B). Rates of this magnitude have been previously observed with other microfluidic liver culture devices in which liver tissue only was cultured as a single tissue [27,31]. The measured metabolic activity remained almost constant over the period of 14 days of co-culture with Caco-2 cells, indicating that sufficient nutrient and gas exchange took place throughout this period.

5) CYP Enzyme Activity

To test the ability of the liver tissue to respond to toxic substances throughout the 14-day co-culture period, we induced the activity of CYP enzymes (CYP 1A1, and CYP 3A4) in the liver chamber on several days after starting the co-culture. We observed that both enzymes were active at levels between 350-500 % of that of cells that were treated with vehicle controls (Fig. 7).

Discussion

1) Modular Approach for Incorporating Tissues from Primary Cell Sources

Accurate predictions of human response obtained from multi-organ microdevices require that the tissues within the devices react authentically to drugs. Authentic tissue behavior can be achieved with advanced tissues that are constructed from primary or stem cell sources, but integrating such advanced tissues into multi-organ microdevices remains a challenge because these tissues require specialized growth conditions to mature to a point where they can be combined with other tissues to create the human metabolism in vitro. To remedy this gap we implemented a modular design where separate tissue-chips were first used to grow and mature each tissue within a specialized environment, and once mature the tissue-chips were combined with each other to yield a multi-organ system. This modular design approach allowed us to combine tissue constructed from a GI tract cell line with liver tissue that was composed of human primary cells. Both tissues require vastly different maturation conditions that can only be achieved in separate growth environments. This achievement is an advantage over previous multi-organ microdevices, where the co-culture of GI tract and liver tissues were demonstrated with tissues constructed from cell lines (Caco-2, HT29 and HepG2/C3A).

We expect that the ability to combine highly advanced tissues constructed from primary or stem cell sources with each other in Body-on-a-chip platforms will render tissue functions and interactions on the platform more physiologic. The liver tissue used here was constructed from a mixture of human primary cells that behave like liver cells would in vivo.[27,30,31] We constructed the liver tissue used in this study from non-parenchymal cells (fibroblasts, stellate cells, Kupffer cells, sinusoidal endothelial cells, and vascular and biliary epithelial cells) and human primary hepatocytes. Such tissues have been shown

to exhibit higher metabolic activity and higher P450 enzyme activity when compared with tissues constructed form cell lines both under static and under fluidic conditions.[27,30,31] In addition, primary liver tissue that contains non-parenchymal cells are also capable of producing interleukins in response to bacterial lipopolycasccaride (LPS), representing one aspect of the immune response not measurable in cell line or hepatocyte-only cultures.[27,30,31]

After a 16-day maturation period for Caco-2 cells and a 9-day maturation period for liver tissue, our platform was capable of maintaining both tissues in co-culture with a common medium for 14 days. Hence day 14 microfluidic device measurements represent sustained tissue longevity for 30-day-old Caco-2 and 23-day-old liver cultures. Low AST concentrations until day 14 (10-17.5 U/L) indicate that liver cells maintained high viability, and suggesting that even longer co-culture times could potentially be achieved in our microfluidic system, analogous to the 90 days sustained function in a static system of same liver tissue.[30] The primary hepatocytes embedded within the 3D liver tissue produced urea and albumin at rates similar to those measured previously in fluidic culture conditions.[27,31] The liver tissue was also capable of responding to CYP enzyme inducers with elevated activities of CYP 1A1 and CYP 3A4 enzymes (350-500% of that of vehicle controls). This activity was slightly higher than what we measured earlier with single-tissue liver cultures within a microfluidic tissue culture platform (i.e. under fluidic flow).[27] This slight increase in activity could be the result of small contributions of activity from Caco-2 cells. Together these data suggest that our platform design was capable of maintaining Caco-2 cell cultures in co-culture with liver tissue constructed from primary cells (human primary hepatocytes and non-parenchymal cells such as fibroblasts, stellate cells, Kupffer cells, sinusoidal endotheliall cells, and vascular and biliary epithelial cells).

The proposed modular design is expandable. Additional single-tissue chips containing additional tissues can be added to the platform without the need for changing the already existing components or the platform itself. Each new chip will contain its own microfluidic channels that connect to the platform in parallel to the already existing tissues.

2) Valves for Creating Unidirectional Medium Flow in Gravity-Driven Flow Devices

Barrier tissues such as the endothelium, the lung epithelium, and the GI tract epithelium are important tissues when testing drug actions. These tissues can significantly alter the bioavailability of drugs in the systemic circulation.[32,33] However, barrier tissues cannot easily be incorporated into low-cost devices that utilize gravity to drive fluidic flow because these devices typically create bidirectional flow that exerts shear forces that periodically changes direction. This type of shear can be detrimental to the barrier function of the tissue because cells constantly re-orient themselves, creating gaps within the tight junctions of the tissue.[34,35] Here, we developed and implemented a passive valve that allowed medium to flow through all organ chambers in one direction and recirculate to the inlet through a separate backflow channel with low hydraulic resistance. This design allowed us to include the GI tract epithelium within a gravity-operated multi-organ microdevice. Although the flow rate is not constant (it changes from zero to its maximum level in each cycle), our measurements show that under unidirectional medium flow TEER values across the GI tract epithelium maintain levels above 250-650 Ωcm2, indicating that the tissue maintained an intact barrier function throughout the 14-day co-culture period with the liver. This is not the case under bidirectional flow, i.e. in devices without valves. The valve allows us to operate low cost, gravity-driven devices with barrier tissues that are sensitive to the direction of shear because it creates unidirectional medium flow, and with that variable, but unidirectional shear.

3) Passive Fluid Control

Gravity-driven Body-on-a-chip devices may pave the way to inexpensive highly parallel operation. We have previously demonstrated this low-cost approach in which medium flow within a single-organ chip is driven via gravity.[24,27] These single-organ systems sustained liver tissue consisting of HepG2/C3A cells for several days,[24] and 3D liver tissue consisting of a mixture of human primary non-parenchymal cells (fibroblasts, stellate cells, Kupffer cells, sinusoidal endothelial cells, and vascular and biliary epithelial cells) and human primary hepatocytes for 21 days.[24,27] However, the medium flow within these systems was significantly higher than it would be for an equivalent tissue volume in the human

body. Such discrepancies between medium flow on chip and blood flow in the body creates on-chip metabolite concentration profiles that are not necessarily physiologic. Here we achieved near-physiologic fluidic flow through each organ chamber (20.5 ± 0.7 μL/min in the liver chamber/basolateral GI tract chamber, compared to physiologic values of 14 μL/min in liver of the same volume as used in the device and 10 μL/min in GI tract tissue of the same size used in the device) by controlling fluid flow passively via the dimensions of the fluidic channels on each tissue chip. The channel's hydraulic resistances passively control the flow rate through each organ chamber. Our device was 3D printed and we expect to yield even more physiologically accurate flow rates when using more precise microfabrication methods when constructing them.

By utilizing the hydraulic resistances to control fluidic flow passively, we maintain a low-cost advantage that only gravity-driven flow systems can provide. In addition, passive fluid control provides operational advantages such as elimination of bubble formation that often interferes with operation in pumped systems.

4) Mimicking Human Physiology

To mimic the human body more completely, more organ compartments need to be incorporated into Body-on-a-chip systems. However, systems that only combine a few tissues plus the blood volume of the entire body can still answer important questions. The GI tract/liver unit is an example of such a subsystem. Combining the GI tract epithelium with liver tissue is of particular interest to us. From the point of view of drug development the GI tract/liver unit is interesting: when drugs are ingested, their rate of transport across the GI tract mucosa and epithelium and the rate of metabolism in the GI tract determine it's concentration profile in the liver, where they are further converted. This first pass conversion can diminish a drug's bioavailability in the blood stream and presents a hurdle to providing effective drug concentrations in the systemic circulation.[36-38] A system that combines GI tract and liver tissues can help in estimating the bioavailability of newly developed drug candidates and drug delivery systems.

When constructing Body-on-a-chip devices that only recreate part of the human body and thereby only part of the human metabolism it is important to consider the following: even though other organs are not represented by actual tissues, their liquid portion such as the blood volume that exists in these organs and within the blood vessels of the human body must be replicated because metabolite concentrations will be diluted within the blood stream. This dilution must be taken into account when designing Body-on-a-chip systems. In our system the medium represents the blood volume of the entire human body (not only the organs represented in the microfluidic system) plus interstitial fluid. However, all multi-organ microdevices published to date contain a liquid portion that is higher than these combined liquid volumes in the human body. This can become a problem when toxic metabolites are diluted and thereby their toxic potential remains undetected. In a gravity-driven system, liquid volumes can be exceptionally low because no tubing or pumping devices have to be filled with medium. The total calculated blood volume in the system presented here (i.e. the blood volume of the entire body scaled down by a factor of 95,000) is 61.3 μL. The total scaled down interstitial fluid volume in our system is 175 μL (based on the assumption that the human body contains about 200 mL of interstitial fluid per kg body weight[39]). To operate our system, we added additional medium. This additional medium volume is 84 μL. It is our goal to decrease the amount of additional liquid in the device so that eventually the liquid-to-cell-volume reaches physiologic levels and metabolite concentrations reach near physiologic values.

An additional consideration for obtaining more accurate predictions of drug action using multi-organ microfluidic devices is the cell density and degree of vascularization within the tissues used. Our in vitro liver tissue consists of a cell culture scaffold, 150,000 non-parenchymal cells, and 250,000 hepatocytes. In vivo tissues of the same volume presumably consist of higher numbers of liver cells, making the overall metabolic conversion within the same tissue volume higher (but similar on a per cell basis). Tissue cell densities must therefore be taken into account when making predictions with multi-organ microdevices.

5) Authenticity of Tissue Behavior

The device we developed here is capable of co-culturing GI tract epithelium constructed from Caco-2 cells with liver tissue constructed from a mixture of human primary cells rather than cells from a cell line or hepatocytes only. The liver tissue was constructed as a 3D tissue from human primary non-parenchymal liver cells (fibroblasts, stellate cells, Kupffer cells, sinusoidal endothelial cells, and vascular and biliary epithelial cells) as well as human primary hepatocytes. Liver tissue constructed from these cells has been shown to be viable in static culture for up to 90 days,[30] making it suitable to test drugs for their effects on the liver under chronic exposure. Another study, in which we placed this liver tissue into a single-organ microfluidic chip and perfused it with medium (bidirectional fluidic flow), showed that fluidic flow activates the tissue, allowing it to reach higher levels of metabolic activity than under static conditions.[27] Here the tissue's metabolic activity reaches similar levels to those observed in the single organ system.

The model of the GI tract epithelium utilized here was constructed from a cell line (Caco-2 cells) because primary GI tract cells are not yet readily available. Caco-2 cells have been shown to differentiate into epithelial cells that establish the physical barrier typical for the GI tract, develop microvilli at their apical surface, and provide the four major routes of nutrient and drug transportation.[40,41] We consider this cell line suitable to mimic the GI tract epithelium, but would like to point out that our GI tract organ chip is suitable for modifications that allow more complex GI tract tissues to be incorporated. For example, the chip could accommodate additional cell types that occur within GI tract tissue, such as goblet cells and M-cells as proposed by Mahler et al.[42] The chip could also support 3D GI tract tissues that aim to replicate the macrovilli that enhance the surface of the GI tract in the human body. Three approaches to recreate such macrovilli have been recently demonstrated.[43-45] In addition, complex systems that aim to recreate the mechanical bowel movement of the GI tract on chip have been developed.[45] Recreating the gut microbioflora provides another opportunity to create a more realistic GI tract.[46,47] All these factors could have an effect on the rate of drug uptake across the GI tract epithelium and could be incorporated into body-on-a-chip systems that combine GI tract tissue with liver tissue for the purpose of assessing the bioavailability of nutrients and drugs.

6) Compatibility with the Drug Development Process

The platform and tissue chips developed for this study are fabricated from 3D printed polymers that were coated with pinhole-free parylene films. Parylene is a biocompatible polymer that does not, unlike silicone materials that are popular in microfluidic device fabrication such as PDMS, absorb or react with metabolites or drugs. The system could be used to test drugs that cannot be tested with PDMS-based systems, particularly those that are hydrophobic and that adsorb to surfaces of devices and tubing.[48]

One of the main advantages of our platform design is that many of these systems can be operated in parallel, making it possible to test many drugs and drug concentrations at the same time. It is quick and easy to assemble and operate the devices because there is no need to connect each inlet/outlet to tubing and pumping equipment. The devices can be placed on rocker platforms to initiate and drive fluidic flow. No further intervention is needed because fluidic flow is controlled entirely passively. Because of the modular design, many organ chips can be loaded with cells and stored in the incubator until they are incorporated into the platform. With exception of the fluidic circuitry, the individual organ chambers on each of the organ chips can be modified to accommodate highly advanced primary tissues and tissues derived from stem cell sources.

Conclusions:

We have developed a two-tissue body-on-a-chip platform that combines GI tract tissue, liver tissue constructed from primary cell sources, and blood surrogate in a near physiologic relationship with each other. The GI tract and the liver represent a subsystem of the human body that determines the uptake and rate of first pass metabolism of orally administered drugs and nutrients. The modular system design allowed us to combine Caco-2 cells with liver tissue constructed from primary cells of human origin. Each tissue was allowed to mature on a separate single-tissue chip before being combined in co-culture for 14 days within a multi-organ device. Our device utilizes gravity to drive fluidic flow, achieves passive flow control via hydraulic resistances of fluidic channels, and contains a set of passive valves that

regulates the direction of fluidic flow. Measurements of urea and albumin production, and of CYP enzyme induction indicate that the liver tissue maintained high levels of metabolic activity and the capacity to react to toxic substances via CYP enzyme activity. TEER values across the Caco-2 cell layer confirm that the cell layer maintains its barrier function throughout the 14-day co-culture period. Our device is a versatile, low-cost approach to building Body-on-a-chip systems. We envision that our technology can be used in settings where many devices need to be assembled and operated in parallel.

Acknowledgement:

Financial support for this work was in part provided by the National Institutes of Health/National Center for Advancing Translational Sciences under grant No. UH2 TR000516-01, and by the National Science Foundation under grant No. CBET-1106153. This work was performed in part at the Cornell NanoScale Science and Technology Facility, a member of the National Nanotechnology Infrastructure Network, which is supported by the National Science Foundation (Grant ECS-0335765). This work also made use of the Nanobiotechnology Center shared research facilities at Cornell.

References:

1 R. Hajar, *Heart Views*, 2011, **12**, 42.
2 M. Allison, *Nature Biotechnology*, 2012, **30**, 41–49.
3 J. Arrowsmith and P. Miller, *Nature Reviews Drug Discovery*, 2013, **12**, 569–569.
4 J. Arrowsmith, *Nature Reviews Drug Discovery*, 2011, **10**, 328–329.
5 H. Olson, G. Betton, J. Stritar and D. Robinson, *Toxicology letters*, 1998, **102-103**, 535–358.
6 P. Perel, I. Roberts, E. Sena, P. Wheble, C. Briscoe, P. Sandercock, M. Macleod, L. E. Mignini, P. Jayaram and K. S. Khan, *BMJ*, 2007, **334**, 197–202.
7 J. Seok, H. S. Warren and A. G. Cuenca, 2013, vol. 110, pp. 3507–3512.
8 M. Leist and T. Hartung, *Arch Toxicol*, 2013, **87**, 563–567.
9 H. R. Ferdowsian and N. Beck, *PloS one*, 2011, **6**, e24059.
10 C. Kilkenny, N. Parsons, E. Kadyszewski, M. F. W. Festing, I. C. Cuthill, D. Fry, J. Hutton and D. G. Altman, *PloS one*, 2009, **4**, e7824.
11 J. M. Perkel, *Science*, 2012, **335**, 1122–1125.
12 C. Zhang, Z. Zhao, N. A. Abdul Rahim, D. van Noort and H. Yu, *Lab on a Chip*, 2009, **9**, 3185–3192.
13 J.-M. Prot, L. Maciel, T. Bricks, F. Merlier, J. Cotton, P. Paullier, F. Y. Bois and E. Leclerc, *Biotechnology and bioengineering*, 2014, **111**, 2027–2040.
14 J.-M. Prot, A. Bunescu, B. Elena-Herrmann, C. Aninat, L. C. Snouber, L. Griscom, F. Razan, F. Y. Bois, C. Legallais, C. Brochot, A. Corlu, M.-E. Dumas and E. Leclerc, *Toxicology and Applied*

Pharmacology, 2012, **259**, 270–280.
15 I. Maschmeyer, A. K. Lorenz, K. Schimek, T. Hasenberg, A. P. Ramme, J. H bner, M. Lindner, C. Drewell, S. Bauer, A. Thomas, N. S. Sambo, F. Sonntag, R. Lauster and U. Marx, *Lab Chip*, 2015, **15**, 2688–2699.
16 I. Maschmeyer, T. Hasenberg, A. Jaenicke, M. Lindner, A. K. Lorenz, J. Zech, L.-A. Garbe, F. Sonntag, P. Hayden, S. Ayehunie, R. Lauster, U. Marx and E.-M. Materne, *Biological Barriers*, 2015, **95, Part A IS -**, 77–87.
17 G. J. Mahler, M. B. Esch, R. P. Glahn and M. L. Shuler, *Biotechnology and bioengineering*, 2009, **104**, 193–205.
18 M. B. Esch, G. J. Mahler, T. Stokol and M. L. Shuler, *Lab on a Chip*, 2014, **14**, 3081–3092.
19 D. A. Tatosian and M. L. Shuler, *Biotechnology and bioengineering*, 2009, **103**, 187–198.
20 K. Viravaidya, A. Sin and M. L. Shuler, *Biotechnology Progress*, 2004, **20**, 316–323.
21 K. Viravaidya and M. L. Shuler, *Biotechnology Progress*, 2004, **20**, 590–597.
22 L. Choucha-Snouber, C. Aninat, L. Grsicom, G. Madalinski, C. Brochot, P. E. Poleni, F. Razan, C. G. Guillouzo, C. Legallais, A. Corlu and E. Leclerc, *Biotechnology and bioengineering*, 2012, **110**, 597–608.
23 S. H. Choi, O. Fukuda, A. Sakoda and Y. Sakai, *Materials Science & Engineering C*, 2004, **24**, 333–339.
24 J. H. Sung, C. Kam and M. L. Shuler, *Lab on a Chip*, 2010, **10**, 446–455.
25 M. B. Esch, A. S. T. Smith, J.-M. Prot, C. Oleaga, J. J. Hickman and M. L. Shuler, *Advanced Drug Delivery Reviews*, 2014, **69-70**, 158–169.
26 Y. Y. Lau, Y.-H. Chen, T.-T. Liu, C. Li, X. Cui, R. E. White and K.-C. Cheng, *Drug Metab. Dispos.*, 2004, **32**, 937–942.
27 M. B. Esch, J.-M. Prot, Y. I. Wang, P. Miller, J. R. Llamas-Vidales, B. A. Naughton, D. R. Applegate and M. L. Shuler, *Lab on a Chip*, 2015, **15**, 2269–2277.
28 B. Davies and T. Morris, *Pharmaceutical Research*, 1993, **10**, 1093–1095.
29 P. S. Price, R. B. Conolly, C. F. Chaisson, E. A. Gross, J. S. Young, E. T. Mathis and D. R. Tedder, *Critical Reviews in Toxicology*, 2003, **33**, 469–503.
30 R. Kostadinova, F. Boess, D. Applegate, L. Suter, T. Weiser, T. Singer, B. Naughton and A. Roth, *Toxicology and Applied Pharmacology*, 2013, **268**, 1–16.
31 M. R. Ebrahimkhani, J. A. S. Neiman, M. S. B. Raredon, D. J. Hughes and L. G. Griffith, *Advanced Drug Delivery Reviews*, 2014, **69-70**, 132–157.
32 K. M. Hillgren, A. Kato and R. T. Borchardt, *Med. Res. Rev.*, 1995, **15**, 83–109.
33 H. Bohets, P. Annaert and G. Mannens, *Current topics in Medical Chemistry*, 2001, **1**, 367–383.
34 J. Iqbal and M. Zaidi, *Biochemical and Biophysical Research Communications*, 2005, **328**, 751–755.
35 P. F. Davies, J. A. Spaan and R. Krams, *Annals of Biomedical Engineering*, 2005, **33**, 1714–1718.
36 K. E. Thummel, D. O'Shea, M. F. Paine, D. D. Shen, K. L. Kunze, J. D. Perkins and G. R. Wilkinson, *Clinical pharmacology and therapeutics*, 1996, **59**, 491–502.
37 B. Wu, K. Kulkarni, S. Basu, S. Zhang and M. Hu, *J. Pharm. Sci.*, 2011, **100**, 3655–3681.
38 L. Z. Benet, C.-Y. Wu, M. F. Hebert and V. J. Wacher, *Journal of Controlled Release*, 1996, **39**, 139–143.
39 K. Aukland and G. Nicolaysen, *ARTICLES | Physiological Reviews*, Physiological reviews, 1981.
40 V. Meunier, M. Bourrié, Y. Berger and G. Fabre, *Cell biology and toxicology*, 1995, **11**, 187–194.
41 P. Artursson, K. Palm and K. Luthman, *Advanced Drug Delivery Reviews*, 2001, **46**, 27–43.
42 G. J. Mahler, M. L. Shuler and R. P. Glahn, *The Journal of nutritional biochemistry*, 2009, **20**, 494–502.
43 M. B. Esch, J. H. Sung, J. Yang, C. Yu, J. Yu, J. C. March and M. L. Shuler, *Biomedical Microdevices*, 2012, **14**, 895–906.

44 J. Yu, S. Peng, D. Luo and J. C. March, *Biotechnology and bioengineering*, 2012, **109**, 2173–2178.
45 H. J. Kim, D. Huh, G. Hamilton and D. E. Ingber, *Lab on a Chip*, 2012, **12**, 2165–2174.
46 C. M. Costello, R. M. Sorna, Y.-L. Goh, I. Cengic, N. K. Jain and J. C. March, *Mol. Pharmaceutics*, 2014, **11**, 2030–2039.
47 J. Yu, R. L. Carrier, J. C. March and L. G. Griffith, *Drug discovery today*, 2014, **19**, 1587–1594.
48 H. Xu and M. L. Shuler, *Biotechnology Progress*, 2009, **25**, 543–551.

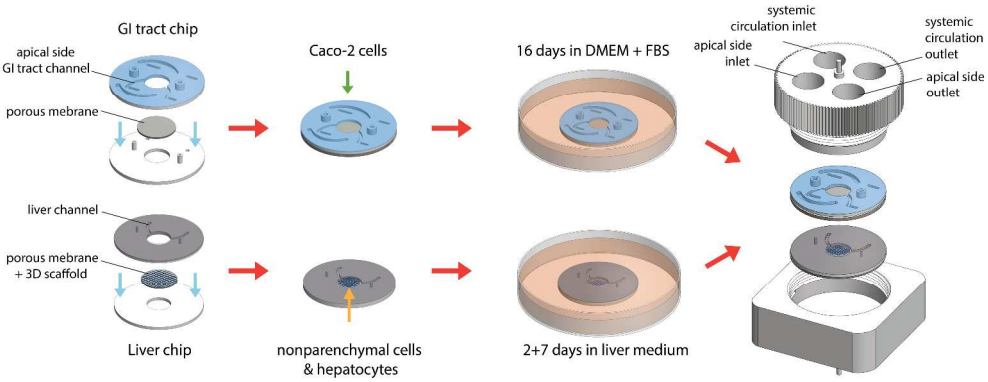

Figure 1: Modular device Design. Each organ chip is seeded with cells that represent the appropriate tissue: Caco-2 cells were seeded onto the GI tract chip 16 days prior to use in the device, and human primary liver cells were seeded 9 days and 2 days before the chips use in the device. Both tissues matured independent of each other before being combined for 14 days of co-culture.

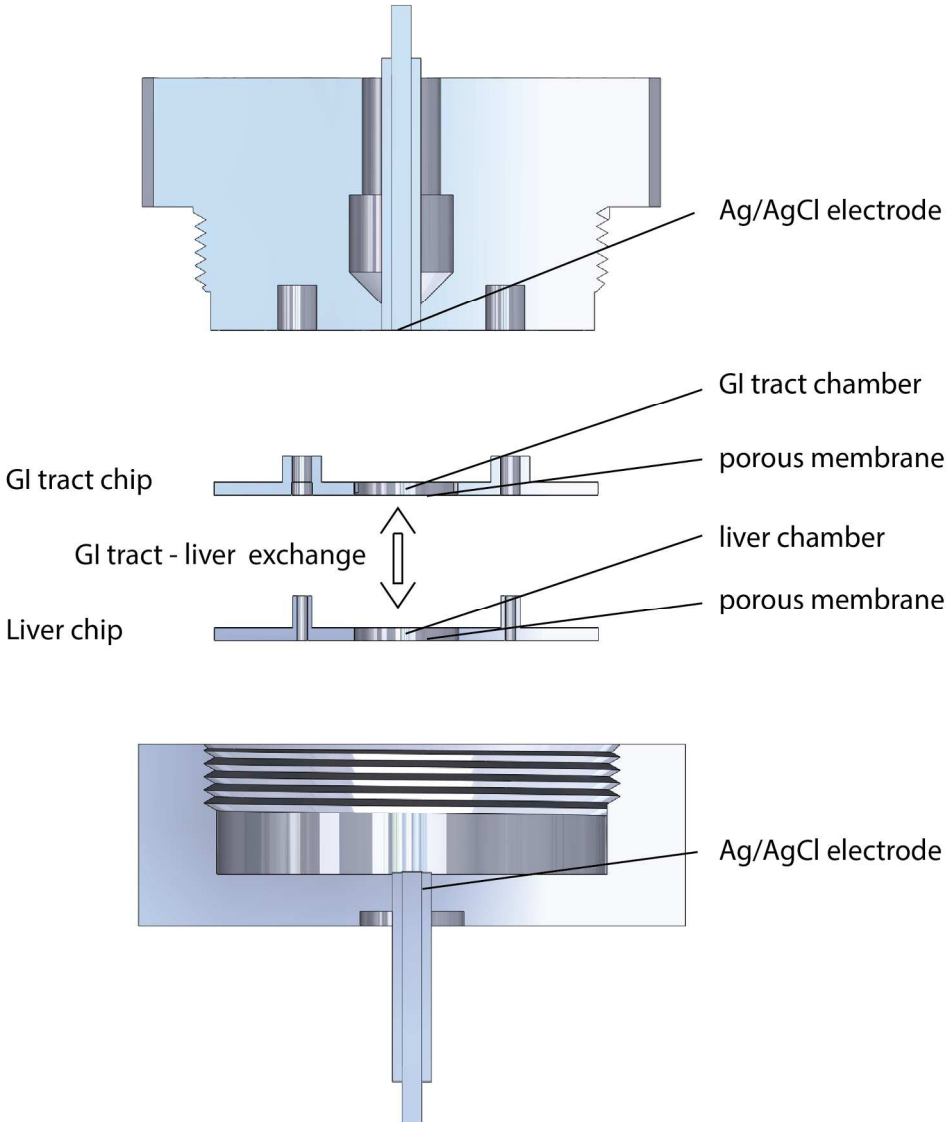

Figure 2: Device Assembly. Shown is a cross section through the middle of the device. Both tissue chips have alignment pins that align them to each other. Mimicking the close relationship between GI tract and liver in the human body, the two tissues can exchange metabolites via a porous membrane. To measure the transepithelial resistance across the GI tract epithelium, we incorporated Ag/AgCl electrodes into the system.

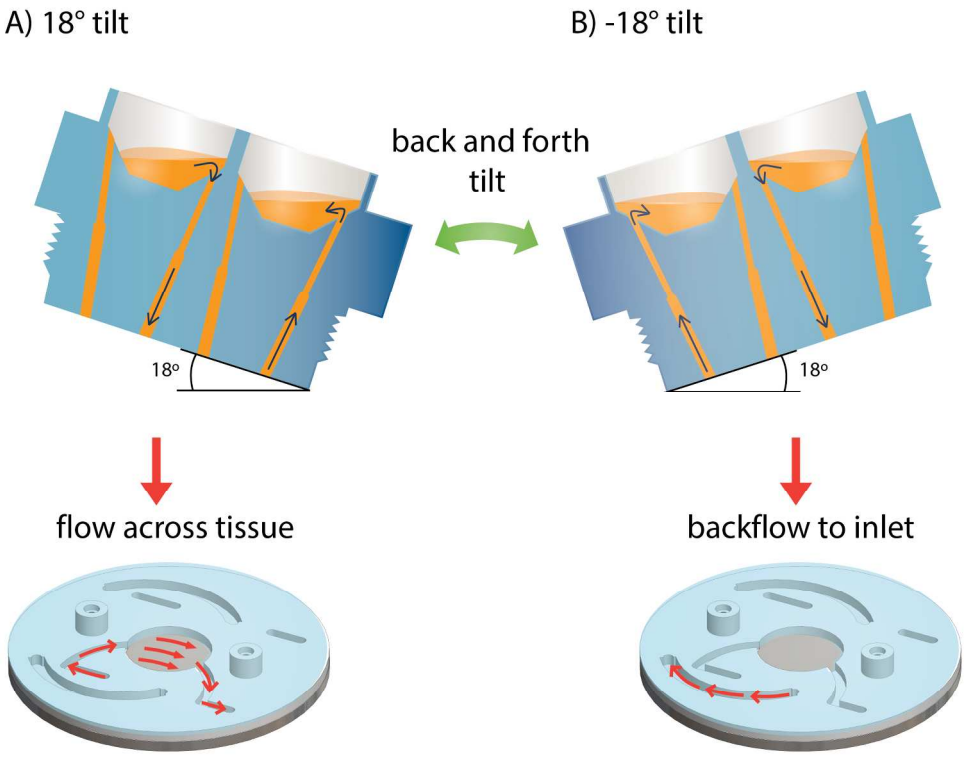

Figure 3: Schematic of the design and operation of the passive valve. Shown is a cross section through the fluidic circuit that supplies the apical side of the GI tract epithelium with medium flow. When tilted at 18º, flow is directed through the tissue culture chamber. When tilted in the opposite direction, flow is limited to the backflow channels. Backflow through the tissue chamber is prevented by capillary forces within the valve capillaries.

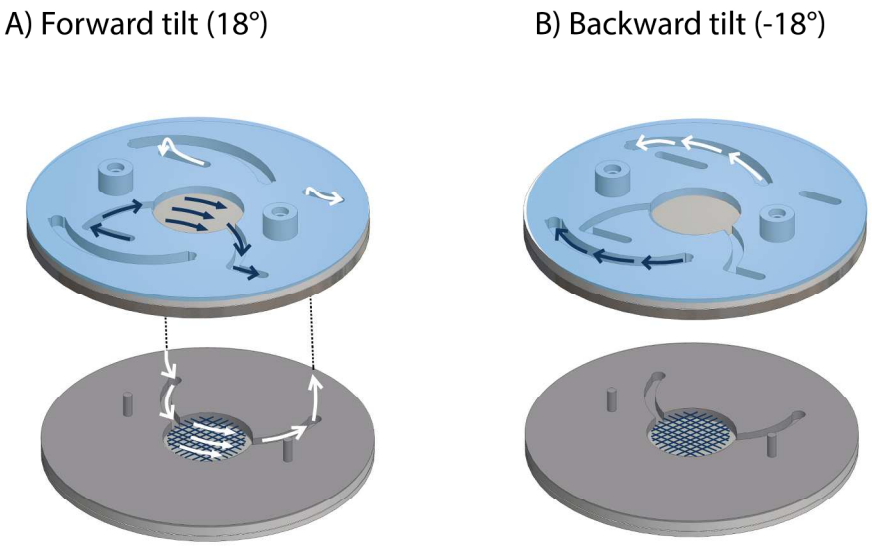

Figure 4: Paths of fluidic flow through the organ chips. When tilted at 18º, flow is directed through the tissue culture chambers (blue arrows show the flow through the apical side of the GI tract and the associated backflow channel and white arrows show the flow through the liver tissue chamber and the associated backflow channel. When tilted at -18º, flow is directed through the backflow channels. The two fluidic circuits do not mix with each other.

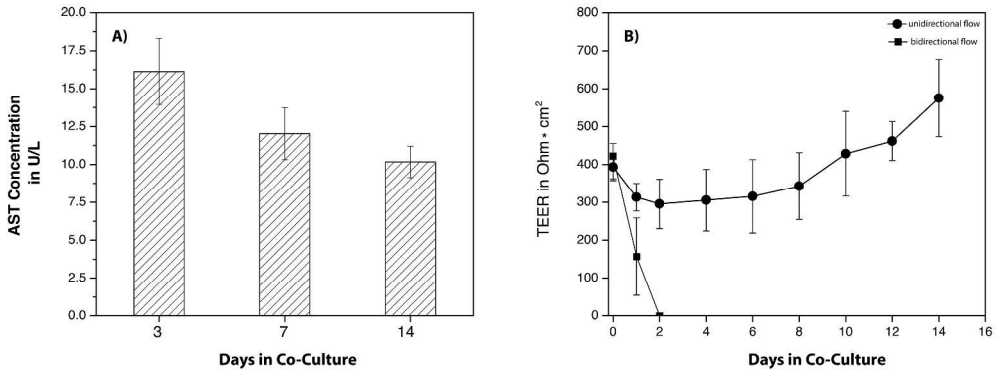

Figure 5: Rates of aspartate aminotransferase (AST) released into the cell culture medium, measured throughout the 14-day microfluidic device co-culture period (A), and TEER across the Caco-2 cell layer measured under unidirectional and bidirectional medium flow throughout the 14-day co-culture period (B). Values are means ± standard deviations, with n = 3 and each separate experiment consisting of two to three technical replicates.

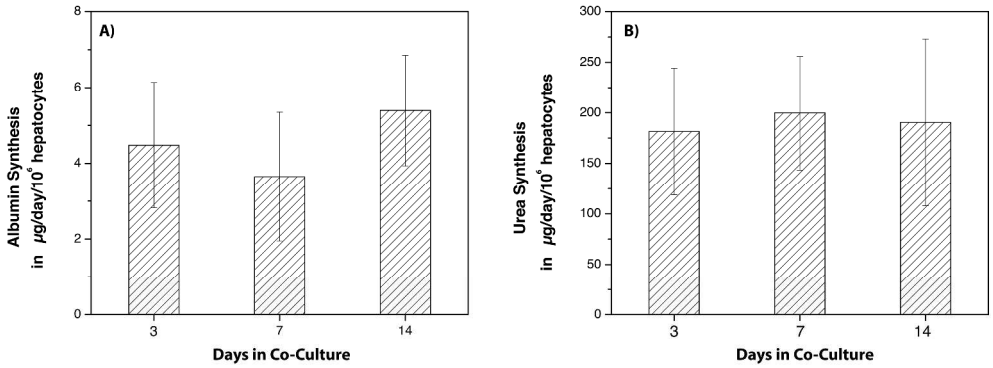

Figure 6: Rates of albumin (A) and urea (B) production throughout the 14-day microfluidic device co-culture period. Values are represented as means ± standard deviations, with n = 3 and each experiment consisting of two to three technical replicates. Significant differences ($P>0.05$) were not detected between the days on which we measured albumin and urea production.

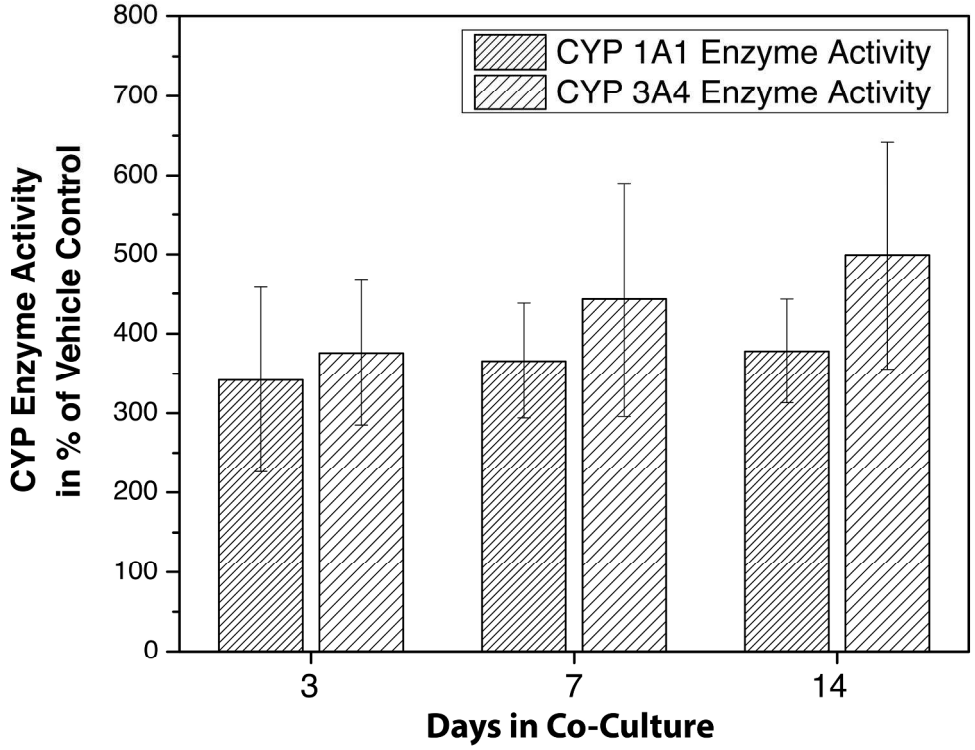

Figure 7: Activity of CYP 1A1 and CYP 3A4 enzymes throughout the 14-day microfluidic device co-culture period. Values are shown as percent increase compared to cultures treated with vehicle controls. Values are means ± standard deviations, with n = 3. Significant differences (P>0.05) between days on which we measure CYP enzyme activity were not detected.